RESEARCH ARTICLE OPEN ACCESS

Development of Cobalt-Erbium nano-ferrites for microwave device applications

Edapalli Sumalatha[1], D. Ravinder[1*]
[1]*Department of Physics, Osmania University, Hyderabad-500007, Telangana, India*
**Corresponding Author: D. Ravinder*

ABSTRACT:
Synthesis of Co-Er nano-ferrites with formulation $CoEr_xFe_{2-x}O_4$ (x = 0, 0.005, 0.010, 0.015, 0.020, 0.025, and 0.030) using technique of citrate-gel auto-combustion, Characterization of prepared powders was done by using XRD, EDS, FESEM and dielectric properties respectively. XRD pattern of CEF nano particles confirm single phase cubic spinal structure. SEM and TEM results reveal homogeneous nature of particles accompanied by clusters having no impurity pickup. TEM analysis gives information about particle size of nanocrystalline ferrites. The observed results can be explained on the basis of composition for microwave device applications.
Key Words: Co-Er nano-ferrites; TEM; XRD; FESEM: Dielectric properties

Date of Submission: 24-01-2021 Date of Acceptance: 08-02-2021

I. INTRODUCTION:

Vigorous research has been accomplished on the fundamental, technological and potential applications of nano-ferrites. Nanomaterials of spinel ferrite have several applications in technology that include magnetic diagnostics and drug delivery[4], potential applications that include high density magnetic information storage devices[1], ferrofluid technology[2], magneto caloric refrigeration[3], magnetic recording media, magnetostriction[5-8], magnetic sensors, microwave devices and electrical generators etc. Ferrites are also used for catalyst and electronic devices. Ferrites are insulators exhibiting various magnetic and electric properties such as low electrical conductivity, dielectric loss, magnetic loss, relative loss factor, moderate dielectric constant, high initial permeability and saturation magnetization.. Doping and thermal changes during synthesis and processing of cobalt-ferrites alter the distribution of metal ions influencing their structure and magnetic properties [6] Citrate-gel auto combustion.

II. EXPERIMENTAL PROCEDURE:

Synthesis of Cobalt-Erbium nano-ferrites with citrate-gel auto combustion technique was taken up with starting materials Cobalt Nitrate (Co (NO3)2·6H2O), Ferric nitrate (Fe (NO3)3·9H2O), Erbium Nitrate (Er (NO3).6H2O), Citric Acid (C6H8O7·H2O) and Ammonia solution (NH3) of 99.9% purity after weighing as per stoichiometric ratio. Later liquification of metal nitrates in distilled water was done and the mixture was stirred at 300 rpm for one hour to obtain a clear homogeneous solution. Next citric acid in aqueous form and metal nitrate was maintained in 1:3 ratio for all samples. Now, ammonia solution was added drop by drop to maintain Ph=7. This solution on stirring was heated at 100 °C temperature for ten to twelve hours to form a viscous gel. The water contained in the mixture gets evaporated slowly to form dry gel generating internal combustion to form a black colored desired sample. This sample was manually grinded and subjected to calcinations at 500°C in furnace for 4 hours. Later these samples in pellet or powder form undergo characterizations with XRD (Bruker, Cu Kα, λ=0.15406nm), Field-emission Scanning Electron Microscope(JEOL JSM-7600 F, Japan) .

Flow chat of Cobalt-Erbium Ferrite

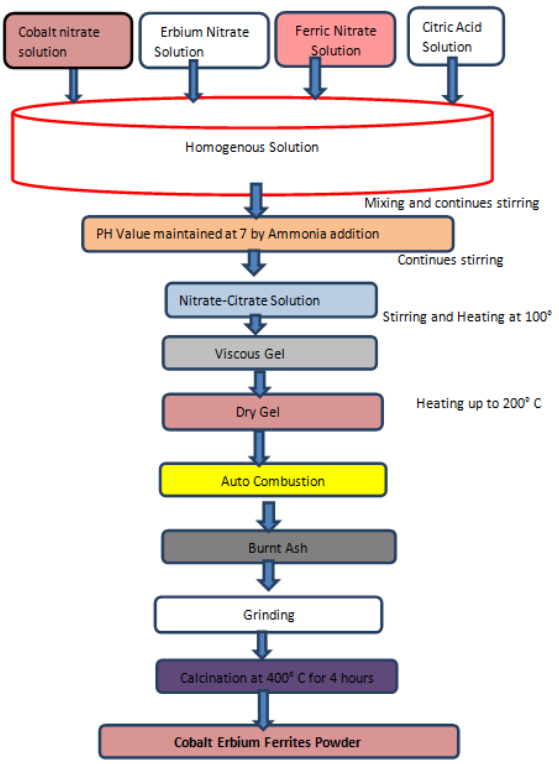

III. ANALYSIS OF XRD:

Figure.1 displays the XRD Rietveld Refinement corresponding to samples of $CoEr_xFe_{2-x}O_4$ with values of x between 0.00 to 0.030 (x= incremented by 0.005). It is observed that the peaks analogous to diffraction planes [111], [320], [311], [400], [511] and [440] match with usual data (JCPDS card no. 022-1086) confirming FCC cubic spinel structure for samples investigated [9,10]. Figure.2 show shift in XRD peaks towards left hand side with increasing concentration of Er^{+3} ions in $CoFe_2O_4$ particles in concurrence with 'a' value. Table.1. lists different parameters of XRD calculated for $CoEr_xFe_{2-x}O_4$ nanoparticles. The values of 'a' were calculated from the equation given [11]

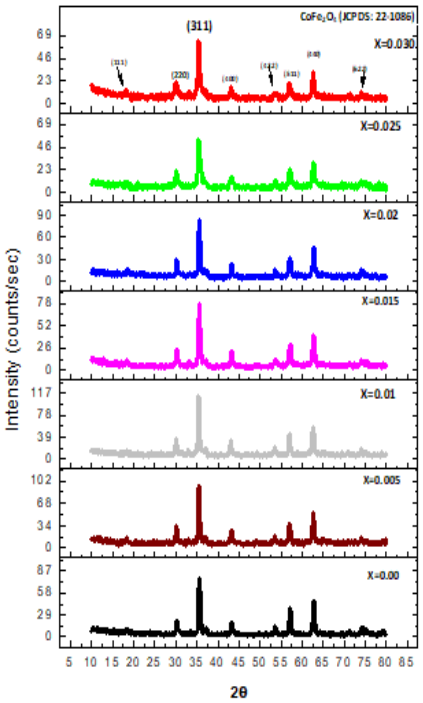

Fig 1: XRD pattern of Co-Er Nano-ferrites

$a= d *(h^2+k^2+l^2)^{1/2}$(1)

where cell constant is given by 'a', inter planer spacing calculated from Bragg's equation ($2\,d\sin\theta = n\lambda$) is denoted by 'd' and miller indices are done by '*h,k,l*'.

It was reported that, low concentration RE (rare earth) doping in spinel ferrite experience phase separation and grain boundary diffusion giving rise to precipitation of additional crystalline phases like hematite($a\text{-}Fe_2O_3$), metal monoxides and orthoferrites($REFeO_3$) [12-15]. Hence in case of rare earth doped ferrites, Er^{+3} doped CFO having no impurity phase ($x \leq 0.010$) is exceptional and is because of auto-combustion. Induced effect due to substitution of erbium on the structure reflects two main observations given by decrease in size of crystal and increase in lattice constant both on small scale. The value of lattice constant slightly enhanced between 8.361 Å to 8.398 Å for x=0.000 to x=0.030 as per Law of Vegard law. Scherrer formula was used to calculate the crystallite size given by (16)

$$L=\frac{0.9*\lambda}{\beta cos\theta}$$

where 'λ' = wavelength of x ray,'β' = peak width at half maximum height and constant 'K' = 0.9. The data related to intense peak (311) was used in estimating size (L). The results indicated reduction in size of crystallite from 20.84nm to 14.40nm (for x=0.0 to 0.030). Further, the high

intense peak (311) shifts towards the lower angle with increasing values of *x* (Figure.2). Table.1 lists the physical parameters obtained from XRD which indicated increase in lattice constant of Co-Fe-Er spinel lattice which might be due to replacement of 8 small Co^{2+} and Fe^{3+} ions with big Er^{3+} ions. Huge difference in radii of these three ions induce strain during formation of lattice and diffusion processes. Requirement of more energy in absorbing RE^{3+} ions with more radii while replacing Fe^{3+} to form RE-O bond decreases crystallization energy and leads to particles of small size. Earlier literature reported similar results on RE-ion substituted cobalt ferrite [17-20]. Therefore, XRD results are liable for expansion of unit cell due to larger Er^{3+} ion doping in CFO. Calculation of X-ray density (*Dx*) was done using:(21)

$$d_x = \frac{8*M}{Na3}$$

where

'M' = composition molecular weight
'*N*'= Avogadro's number
'*a*'= lattice constant.

Table 1: Lattice constant, Crystallite Size and X-ray density of Co-Er nano-ferrites

Compositions	Lattice Constant(A)	Crystallite Size (nm)	X-ray density(dx) (gcm−3)
$CoFe_2O_4$	**8.361**	**20.84**	**5.3344**
$CoEr_{0.005}Fe_{1.995}O_4$	**8.367**	**20.43**	**5.3356**
$CoEr_{0.010}Fe_{1.990}O_4$	**8.373**	**19.19**	**5.3367**
$CoEr_{0.015}Fe_{1.985}O_4$	**8.379**	**19.02**	**5.3379**
$CoEr_{0.020}Fe_{1.980}O_4$	**8.386**	**17.73**	**5.3370**
$CoEr_{0.025}Fe_{1.975}O_4$	**8.392**	**15.56**	**5.3381**
$CoEr_{0.030}Fe_{1.970}O_4$	**8.398**	**14.40**	**5.3392**

X-ray density value is found to increase from 5.3344gm/cm3 to 5.3392gm/cm3 (*x* = 0.00 to *x* =0.030) with increasing Er^{3+} content. The bulk density increased from 3.2113 to 3.2141(x=0.00 to x=0.030). At the same time, $CoFe_{2-x}Er_xO_4$ ceramics having more Er content (x=0.015) exhibited lower $ErFeO_3$ orthoferrite amount along with primary spinel ferrite phase. Cobalt ferrite in inverse spinel form has tetrahedral site occupied by half of Fe^{+3} while the remaining half of Fe^{+3} and Co^{-2} occupy octahedral sites[22]. Any change in site occupation of Fe^{+3} and Co^{-2} might be because of preparation technique and affect cell constant. Bulk densities were found from the relation [23].

IV. FIELD EMISSION SCANNING ELECTRON MICROSCOPY (FE-SEM)

Figure 2. shows studies on surface morphology of ferrite powders with the help of FE-SEM. The nature of ferrite particle in the samples is uniform indicating fine form of agglomeration and grain growth. Agglomerate formation specifies strong magnetic nature of erbium doped ferrites. These studies also confirm microstructure changes on doping Er^{+3}. A close look at these microstructures indicate improvement in microstructure and spherical shaped grains in all samples. Apart from this Erbium doping increases percentage of porosity in small range between 39.8001to 39.8018 illustrating individual grains and grain boundaries are separated.

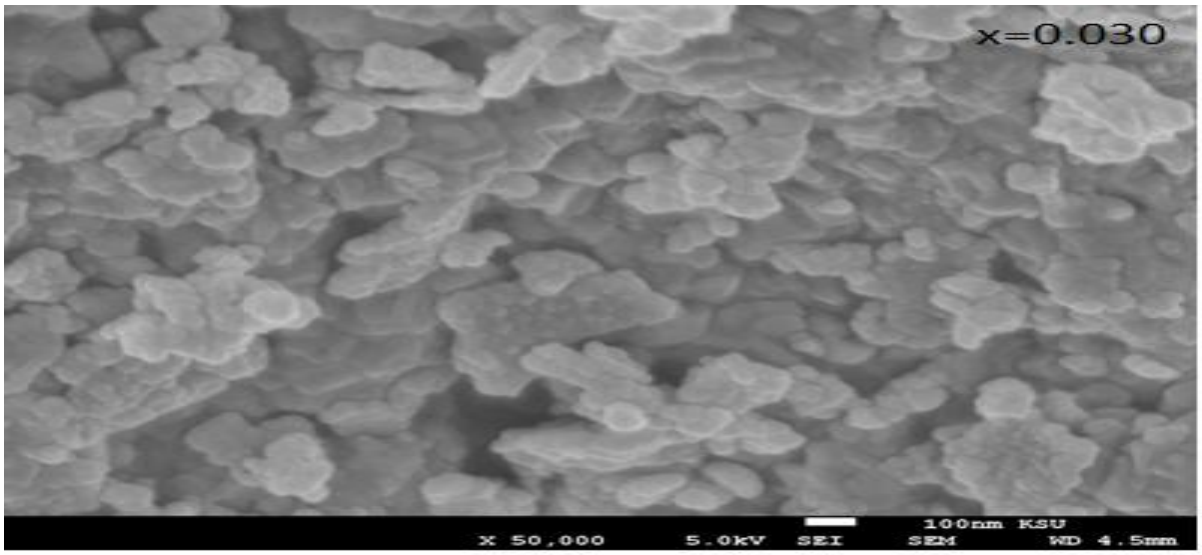
x=0.030
X 50,000 5.0kV SEI SEM 100nm KSU WD 4.5mm

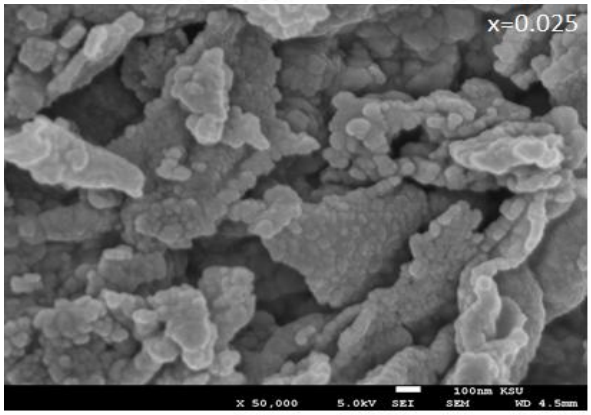
x=0.025
X 50,000 5.0kV SEI SEM 100nm KSU WD 4.5mm

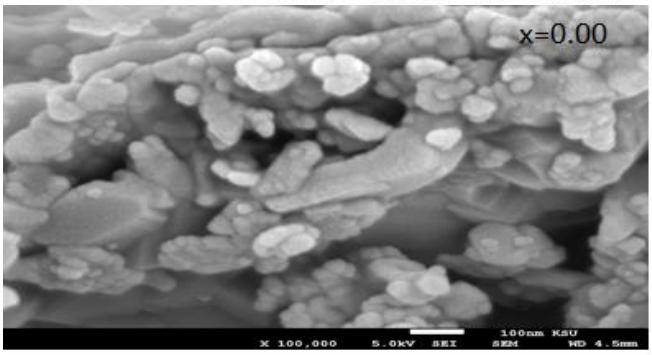
x=0.00
X 100,000 5.0kV SEI SEM 100nm KSU WD 4.5mm

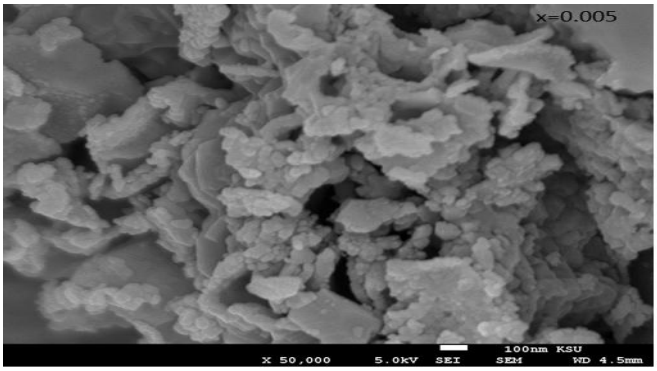
x=0.005
X 50,000 5.0kV SEI SEM 100nm KSU WD 4.5mm

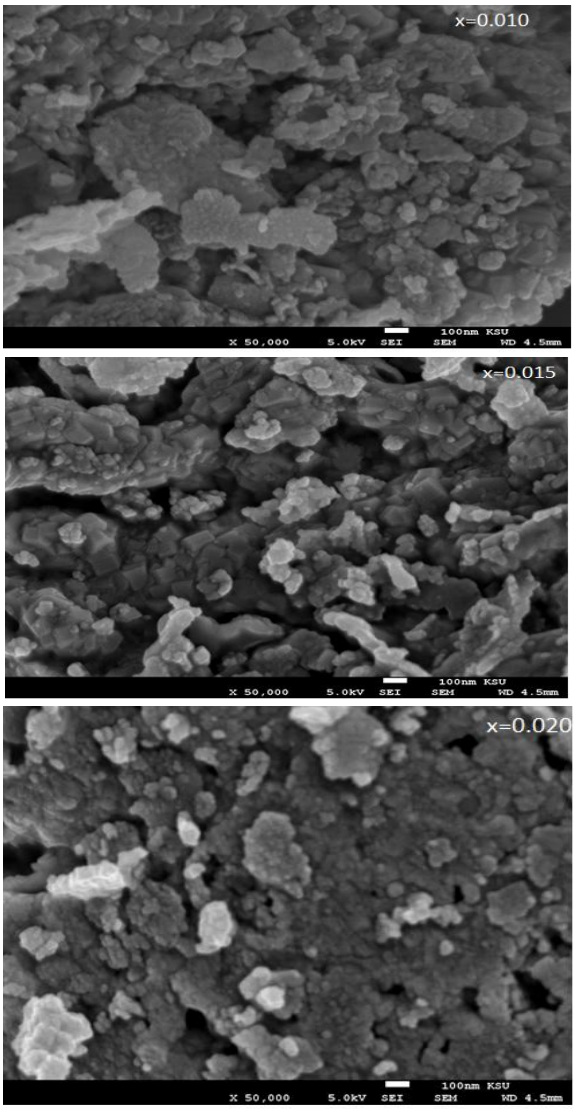

V. DIELECTRIC PROPERTIES ANALYSIS:

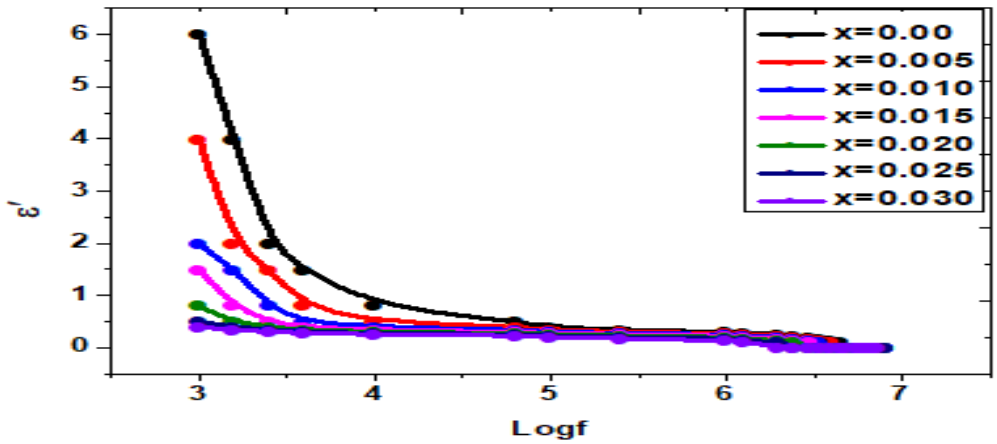

Fig 3.: Variation of Dielectric constant with frequency for Co-Er nano-ferrites

The dielectric properties study for the ferrite nanoparticles supply us information about the electrical conduction mechanism in terms of the dielectric response in applied AC electric field. When ac field applied to the two sides of a dielectric specimen it gets polarized, this polarization changes the dielectric constant of the substance. Due to the temporal phase shift in driving force and the resulting polarization, a loss in the current component takes place which is the cause of tangent loss of the samples. Ferroelectric substances are generally identifying their dielectric loss angle and dielectric constant. The dielectric tangent loss, and the constant of the materials depends on the frequency of the applied voltage and also on temperature, preparation method, chemical composition, stoichiometry, porosity, ionic charge, grain size, and cation distribution between the tetrahedral and octahedral structures[17]. In the present study, pellet capacitance, dielectric loss angle (tan δ) and air capacitance with pellet thickness were measured using LCR meter at room temperature. The real part of the dielectric constant (ε'), and imaginary part of the dielectric constant (ε") has been computed from the following equation

$$\varepsilon' = \frac{C_P d}{\varepsilon_0 A}$$

$$\varepsilon'' = \varepsilon' \tan\delta$$

where

C = pellets capacitance (farads), d = pellets thickness (meters), A=pellets cross-sectional area, ε_o = free space permittivity constant, and f is frequency. Fig.3 & 4 shows the behavior of dielectric constant and dielectric loss with varying frequency. The dielectric values have been given in Table.2. It can be seen from the table that the low values dielectric constant and dielectric loss can be design for microwave devices such Oscillators, Phase shifters and gyrators. The dielectric loss tangent reduces with increased frequency. The stored energy is described by dielectric constant (ε') which is high in low frequency range and decrease with increasing frequency and ultimately reaches minimum at higher frequency which is the normal behavior in most of the ferrite materials. This behavior was observed in the present work on Er-Co ferrites[24, 25].

Table.2: The Variation of Dielectric constant (ε) and Dielectric loss factor For Co-Er nano-ferrites.

Composition	**ε' at 1k Hz**	**ε″at 1k Hz**	**tanδ at 1k Hz**
X=0	15	95	0.045
X=0.01	12	30	0.03
x=0.020	8	18	0.025
X=0.030	5	0.7	0.05

This variation is because of high ε' value at less frequency due to presence of different polarizations that decrease with increasing frequency[26]. Decrease in dielectric constant with increase in frequency, at higher frequencies effecting polarization to lag behind the applied field to result in low dielectric constant because of electric polarizability[27]. The present study indicated and nicely correlate with previous report [24]. The dielectric loss represents the energy dissipation in a dielectric material and is defined in terms of dielectric loss angle (tan δ) and dielectric loss factor (ε"). This is developed because of impurities and crystal imperfections in the material that leads to polarization lagging behind applied field[28, 29]. Fig. 3 and 4, shows the variation of dielectric loss angle and factor respectively as a function of frequency at room temperature and summarized in Table 2. It can be seen that the dielectric loss angle (tan δ) and dielectric loss factor (ε") decreases with frequency increase, a normal behavior of any ferrite material and then become constant at high values. Decreasing of tan δ and ε" with frequency was explained by Maxwell–Wagner model and Koop's theory . A small amount of energy is required in high frequency region (low resistivity) for hoping of electrons between Fe^{2+} and Fe^{3+} ions at B site while in low frequency region (high resistivity) large amount of energy. Hence two layer type explains the dielectric behavior of ferrite samples under investigation [29].

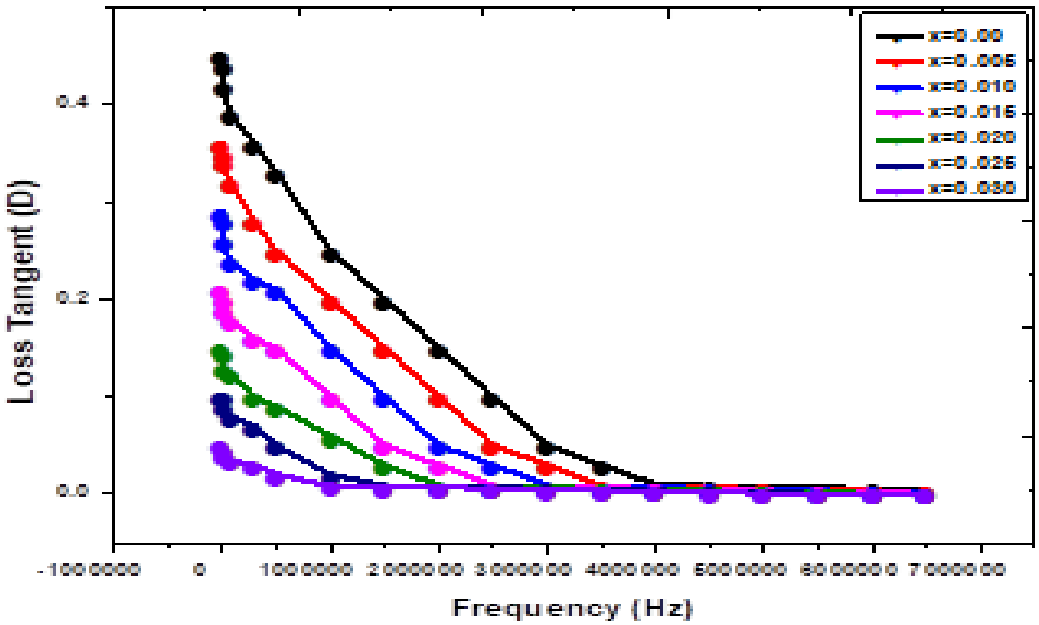

Fig 4: Variation of Dielectric Loss tangent with frequency for Co-Er nano- ferrites.

The values of tan δ and ε" are found to be high for un doped cobalt ferrite (x=0.00) and decrease for x=0.005 to 0.030 with increasing Er-substitution. This makes them possible materials for applications at high frequency. Replacement of iron with erbium decreases dielectric loss are shown in Figure [12,13,14]. It is a known fact that defects are more in interfacial regions when compared to intrinsic grain regions. The prevention of surface conduction due to doping of Er in cobalt ferrite may reduce dielectric loss in the overall spectrum which was observed[8, 13], indicating very low signal loss while passing through these materials. The dielectric loss angle also depends on stoichiometry, Fe^{2+} content, and structural homogeneity which in turn depend upon the composition and sintering temperature of the samples.

VI. CONCLUSIONS

Synthesis and characterization of erbium substituted cobalt ferrites along with conglomeration was done using citrate-gel auto combustion method. Significant induced effect of Erbium was observed on the structure of crystal structure, dielectric constant, morphology and electrical transport properties of cobalt ferrite material. The crystallite size was decreased from 20.84nm-14.40nm. According to the SEM analysis the growth in grain along with agglomeration form was found for all samples. The low values dielectric constant and dielectric loss can be design for microwave devices such Oscillators, Phase shifters and gyrators.

ACKNOWLEDGMENTS:

Thanks to CSIR, New Delhi, India for Research Fellowship (CSIR-JRF). The authors are grateful to the Prof. Syed Rahman, Head Department of Physics, University College of Science, Osmania University Hyderabad for his constant encouragement.

Electronic Materials & Nanomagnetism Lab,
Department of Applied Physics, Amity School of Applied Sciences, Amity University Haryana, Gurgaon, 122413, In

REFERENCES:

[1]. Song Q, Zhang ZJ (2004) Shape Control and Associated Magnetic Properties of Spinel Cobalt Ferrite Nanocrystals. J. Am. Chem. Soc. 2004, 126, 19, 6164–6168 https://pubs.acs.org/doi/10.1021/ja049931r

[2]. Vinosha PA, Das SJ (2018) Investigation on the role of pH for the structural, optical and magnetic properties of cobalt ferrite nanoparticles and its effect on the photo-fenton activity. Materials Today: Proceedings 5:8662-8671 https://www.sciencedirect.com/science/article/pii/S2214785317332807

[3]. Vázquez-Vázquez C, Lovelle M, Mateo C, López-Quintela MA, Buján-Núñez MC, Serantes D, Baldomir D, Rivas J (2008) Magnetocaloric effect and size-dependent study of the magnetic properties of cobalt ferrite nanoparticles prepared by solvothermal synthesis. Wiley Online

Library:205:1358-1362 https://doi.org/10.1002/pssa.200778128

[4]. Habiba AH, Ondeck CL, Chaudhary P, Bockstaller MR, McHenry ME (2008) Evaluation of iron-cobalt/ferrite core-shell nanoparticles for cancer thermotherapy. Journal of Applied Physics 103:07A307 https://doi.org/10.1063/1.2830975

[5]. Nlebedim IC, Hadimani RL, Prozorov R, Jiles DC (2013) Structural, magnetic, and magnetoelastic properties of magnesium substituted cobalt ferrite. Journal of Applied Physics 113:17A928 https://doi.org/10.1063/1.4798822

[6]. Cullity BD, Graham CD (2009) Introduction to Magnetic Materials, 2nd Edition. Wiley-IEEE Press 568 Pages https://www.wiley.com/en-in/Introduction+to+Magnetic+Materials%2C+2nd+Edition-p-9780471477419

[7]. Weiss A (1975) Craik (Ed.) DJ (1975) Magnetic Oxides, Parts 1 and 2 (John Wiley & Sons, Bristol, 1975). Wiley Online Library 80:175-175 https://doi.org/10.1002/bbpc.19760800218

[8]. Prathapani S, Jayaraman TV, araprasadarao EK, Das D (2014) Structural and ambient/sub-ambient temperature magnetic properties of Er-substituted cobalt-ferrites synthesized by sol-gel assisted auto-combustion method, Journal of Applied Physics. Journal of Applied Physics 116:023908 https://doi.org/10.1063/1.4889929

[9]. Heiba ZK, Mohamed MB, Arda L, Dogan N (2015) Cation distribution correlated with magnetic properties of nanocrystalline gadolinium substituted nickel ferrite. Journal of Magnetism and Magnetic Materials 391:195-202 https://doi.org/10.1016/j.jmmm.2015.05.003

[10]. Kambale RC, Shaikh PA, Kamble SS, Kolekar YD (2009) Effect of cobalt substitution on structural, magnetic and electric properties of nickel ferrite. Journal of Alloys and Compounds 478:599-603 https://www.sciencedirect.com/science/article/abs/pii/S0925838808021257

[11]. Dobrott RD (1959) Elements of X-ray Diffraction, Addison-Wesley, London. Characterization of Solid Surfaces pp:147-178 https://link.springer.com/chapter/10.1007/978-1-4613-4490-2_8

[12]. Andreu I, Natividad E, Ravagli C, Castroa M, Baldib G (2014) Heating ability of cobalt ferritenanoparticles showing dynamic and interaction effects. RSC Adv., 2014,4, 28968-28977 https://doi.org/10.1039/C4RA02586E

[13]. Kakade SG, Ma Y, Devan RS, Kolekar YD, Ramana CV (2016) Dielectric, Complex Impedance, and Electrical Transport Properties of Erbium (Er3+) Ion-Substituted Nanocrystalline Cobalt-Rich Ferrite. J. Phys. Chem. C 2016, 120, 10, 5682–5693 https://pubs.acs.org/doi/abs/10.1021/acs.jpcc.5b11188

[14]. Park K, Hwang HK (2013) Fabrication and electrical properties of nanocrystalline Dy3+-doped CeO2 for intermediate-temperature solid oxide fuel cells. Energy 55:304-309 https://doi.org/10.1016/j.energy.2013.04.017

[15]. Kumar H, Singh JP, Srivastava RC, Negi P, Agrawal HM, Asokan K (2014) FTIR and electrical study of dysprosium doped cobalt ferrite nanoparticles. https://doi.org/10.1155/2014/862415

[16]. Hashim M, Alimuddin, Kumar S, Shirsath SE, Kotnala RK, Shah J, Kumar R (2012) synthesis and characterization of nickel substuded cobalt ferrite. Materials Chemistry and Physics 139:364-374 https://doi.org/10.1016/j.matchemphys.2012.09.019

[17]. Wu Y, Li J, Bai H, He S, Hong Y, Shi K, Zhou Z (2018) Colossal Dielectric Behavior and Dielectric Relaxation of (Li, Fe) Co-Doped ZnO Ceramics. Wiley Online Library:Rapid Research Letter 12:1800126 https://onlinelibrary.wiley.com/doi/abs/10.1002/pssr.201800126

[18]. Salunkhe AB, Khot VM, Phadatare MR, Thorat ND, Joshi RS, Yadav HM, Pawar SH (2013) Low temperature combustion synthesis and magnetostructural properties of CoMnnano-ferrites. Journal of Magnetism and Magnetic Materials 352:91-98 https://doi.org/10.1016/j.jmmm.2013.09.020

[19]. Rus SF, Vlazan P, Herklotz A (2016) Synthesis and characterization of Zirconium substituted cobalt ferrite nanopowders. Journal of Nanoscience and Nanotechnology 16:1 https://www.osti.gov/pages/servlets/purl/1324165

[20]. Rathore D, Kurchania R, Pandey RK (2014) Influence of particle size and temperature on the dielectric properties of CoFe2O4 nanoparticles. International Journal of Minerals, Metallurgy, and Materials 21:408–414 https://link.springer.com/article/10.1007/s12613-014-0923-8

[21]. Rahman MT, Ramana CV (2014) Impedance spectroscopic characterization of gadolinium substituted cobalt ferrite ceramics. Journal of Applied Physics 116:164108 https://doi.org/10.1063/1.4896945

[22]. Goldman A (2006) Modern Ferrite Technology, 2nd ed. Ferrite Technology Pittsburgh, PA, USA https://download.e-bookshelf.de/download/0000/0009/50/L-G-0000000950-0002340313.pdf

[23]. Raghasudha M, Ravinder D, Veerasomaiah P (2003) FTIR Studies and Dielectric Properties of Cr Substituted Cobalt Nano Ferrites Synthesized by Citrate-Gel Method. Nanoscience and Nanotechnology 2013, 3(5): 105-114 https://www.researchgate.net/publication/271907985_FTIR_Studies_and_Dielectric_Properties_of_Cr_Substituted_Cobalt_Nano_Ferrites_Synthesized_by_Citrate-Gel_Method

[24]. Kolekar YD, Sanchez LJ, Ramana CV (2014) Dielectric relaxations and alternating current conductivity in manganese substituted cobalt ferrite. Journal of Applied Physics 115:144106 https://aip.scitation.org/doi/10.1063/1.4870232

[25]. Ahmad R, Gul IH, Zarrar M, Anwar H, Niazi MBK, Khan A (2016) Improved electrical properties of cadmium substituted cobalt ferrites nano-particles for microwave application. Journal of Magnetism and Magnetic Materials 405:28-35 https://www.sciencedirect.com/science/article/abs/pii/S0304885315308854

[26]. Kakade SG, Kambale RC, Kolekar YD, Ramana CV (2016) Dielectric, Electrical Transport and Magnetic Properties of Er3+Substituted Nanocrystalline Cobalt Ferrite. Journal of Physics and Chemistry of Solids 98:20-27 https://www.sciencedirect.com/science/article/abs/pii/S0022369716300580

[27]. Jabez S, Mahalakshmi S, Nithiyanantham S (2017) Frequency and temperature effects on dielectric properties of cobalt ferrite. Journal of Materials Science: Materials in Electronics 28:5504–5511 https://link.springer.com/article/10.1007/s10854-016-6212-8

[28]. Jonker GH (1959) Analysis of the semiconducting properties of cobalt ferrite. Journal of Physics and Chemistry of Solids 9:165-175 https://www.sciencedirect.com/science/article/abs/pii/0022369759902069

[29]. Kambale RC, Shaikh PA, Bhosale CH, Rajpure KY, Kolekar YD (2009) The effect of Mn substitution on the magnetic and dielectric properties of cobalt ferrite synthesized by an autocombustion route. Smart Materials and Structures 18:115028 https://iopscience.iop.org/article/10.1088/0964-1726/18/11/115028/meta